J|A|C|S ARTICLES

Published on Web 02/09/2010

Plasmonic Field Enhancement of the Exciton−Exciton Annihilation Process in a Poly(*p*-phenyleneethynylene) Fluorescent Polymer by Ag Nanocubes

Mahmoud A. Mahmoud,[†] Adam J. Poncheri,[†] Ronnie L. Phillips,[‡] and Mostafa A. El-Sayed*,[†]

Laser Dynamics Laboratory, School of Chemistry and Biochemistry, Georgia Institute of Technology, Atlanta, Georgia 30332-0400

Received September 16, 2009; E-mail: melsayed@gatech.edu

Abstract: Using the Langmuir−Blodgett (LB) technique, a poly(paraphenyleneethynylene) (PPE) fluorescent conjugated polymer was assembled on either a quartz substrate (system I) or on the surface of silver nanocube (AgNC) monolayers (system II). The fluorescence intensity of the polymer was studied in system I as a function of the surface density of the polymer sample when deposited on quartz substrates and in system II on the surface coverage of the underlying AgNC monolayers. In system I, a continual increase in the fluorescence intensity is observed as the surface density of excited polymer is increased. In system II, the fluorescence intensity of the polymer first increased until a threshold surface coverage of AgNC was reached, after which it decreased rapidly with increasing surface coverage in the AgNC monolayer. The exciting light intensity dependence is studied before and after this threshold in system II. The results suggest that one-photon processes were responsible for the increased intensity before the threshold, and two-photon processes were responsible for the rapid decrease in the polymer fluorescence intensity after the threshold. These observations are explained by the increase of the surface plasmon enhancement of the exciting light intensity as the nanoparticle surface coverage is increased. In turn, this increases the polymer absorption rate, which results in a continuous increase in the exciton density and is evident by an increase in the fluorescence intensity. At the threshold, the increased exciton density leads to an increase in the rate of exciton−exciton collisions, which leads to exciton−exciton annihilations. When this phenomenon becomes faster than the rate of fluorescence emission, an intensity decrease is observed. By exploiting the surface plasmon enhancement of absorption processes, we have observed the first exciton−exciton annihilation using a low-intensity Hg-lamp continuous wave source.

Introduction

Noble (plasmonic) metallic nanoparticles have been used in such applications as catalysis,[1] sensing,[2−4] drug delivery,[5,6] and the potential diagnosis and in vivo treatment of cancer.[7−9] The great versatility of these particles comes from the ability to fine-tune their physical, optical, and photothermal properties.[10−14] Metallic nanoparticles can adopt a wide range of sizes and shapes (spheres,[1] rods,[15] cages,[16] cubes,[17,18] etc.), which in turn give rise to an even wider range of spectral properties (single or multiple surface plasmon resonance (SPR) peaks from the UV to the NIR).

The ability to generate surface plasmon resonances (SPR) upon resonant light excitation separates metallic nanoparticles from other nanomaterials. When these nanoparticles are irradiated with electromagnetic radiation of the appropriate wavelength, surface plasmon resonance of the conduction band electrons takes place and induces strong electromagnetic fields

[†] Laser Dynamics Laboratory, School of Chemistry and Biochemistry.
[‡] School of Chemistry and Biochemistry.

(1) Freund, P. L.; Spiro, M. *J. Phys. Chem.* **1985**, *89*, 1074.
(2) Jin, R.; Wu, G.; Li, Z.; Mirkin, C. A.; Schatz, G. C. *J. Am. Chem. Soc.* **2003**, *125*, 1643.
(3) Haes, A. J.; Chang, L.; Klein, W. L.; Van Duyne, R. P. *J. Am. Chem. Soc.* **2005**, *127*, 2264.
(4) Berger, C. E. H.; Beumer, T. A. M.; Kooyman, R. P. H.; Greve, J. *Anal. Chem.* **1998**, *70*, 703.
(5) Brigger, I.; Dubernet, C.; Couvreur, P. *Adv. Drug Delivery Rev.* **2002**, *54*, 631.
(6) Aymonier, C.; Schlotterbeck, U.; Antonietti, L.; Zacharias, P.; Thomann, R.; Tiller, J. C.; Mecking, S. *Chem. Commun. (Cambridge, U. K.)* **2002**, 3018.
(7) El-Sayed, I. H.; Huang, X. H.; El-Sayed, M. A. *Nano Lett.* **2005**, *5*, 829.
(8) Loo, C.; Lowery, A.; Halas, N.; West, J.; Drezek, R. *Nano Lett.* **2005**, *5*, 709.
(9) Fortina, P.; Kricka, L. J.; Graves, D. J.; Park, J.; Hyslop, T.; Tam, F.; Halas, N.; Surrey, S.; Waldman, S. A. *Trends Biotechnol.* **2007**, *25*, 145.
(10) Link, S.; El-Sayed, M. A. *Int. Rev. Phys. Chem.* **2000**, *19*, 409.
(11) Jain, P. K.; Huang, X. H.; El-Sayed, I. H.; El-Sayed, M. A. *Acc. Chem. Res.* **2008**, *41*, 1578.
(12) Grzelczak, M.; Perez-Juste, J.; Mulvaney, P.; Liz-Marzan, L. M. *Chem. Soc. Rev.* **2008**, *37*, 1783.
(13) Perez-Juste, J.; Pastoriza-Santos, I.; Liz-Marzan, L. M.; Mulvaney, P. *Coord. Chem. Rev.* **2005**, *249* (17-18), 1870.
(14) Kreibig, U.; Vollmer, M. *Optical Properties of Metal Clusters*; Springer Series in Materials Science 25; Springer: New York, 1995.
(15) Nikoobakht, B.; El-Sayed, M. A. *Chem. Mater.* **2003**, *15*, 1957.
(16) Yen, C. W.; Mahmoud, M. A.; El-Sayed, M. A. *J. Phys. Chem. A* **2009**, *113*, 4340.
(17) Sun, Y. G.; Xia, Y. N. *Science* **2002**, *298*, 2176.
(18) Mahmoud, M. A.; El-Sayed, M. A. *J. Phys. Chem. C* **2008**, *112*, 14618.

on and around the particle surface.[10,19,20] This leads to an enhancement in the radiative and nonradiative electronic properties of the nanoparticles themselves, as well as nearby electronic systems. The near-field effects enhance the absorption and scattering processes by amplifying the electromagnetic fields of the resonant exciting light. Surface enhanced Raman spectroscopy (SERS) results from the near-field plasmonic enhancement of the Raman scattering spectrum of adsorbed molecular systems.[21−23] Enhanced Rayleigh scattering by plasmonic fields has also been use in dark-field scattering for medical diagnosis.[24] Fluorescence of nearby molecules can be enhanced at distances from the surface that are large enough to minimize electron transfer quenching mechanisms but close enough to feel the surface plasmon near-fields of the plasmonic nanoparticles. The near-field plasmonic effects on the nonradiative processes have also been demonstrated in studies within our group, such as the nonradiative electronic relaxation in the semiconductor of CdTe−Au core−shell nanorods[25] and on the rates of retinal photoisomerization[26] and the proton pump process[27] in the photosynthetic system of bacteriorhodopsin. In most of these systems, the mechanisms involved are found to be blamed on the great enhancements of the radiative transitions in resonance with the plasmonic frequency. In the present contribution, we report additional evidence that the plasmonic near-field of silver nanocubes also induces the nonradiative exciton−exciton annihilation processes in a nearby conjugated polymer at low excitation light intensities due to the enhancement of its singlet state excitation.

As two or more nanoparticles are brought into close proximity, their surface plasmon fields couple to produce enhanced fields between the particles and a characteristic red-shift in their SPR bands.[28−31] Electron beam and nanosphere lithography have been used extensively to fabricate and arrange metal nanoparticles for studying the distance dependence of these coupled field effects.[28−30,32,33] An alternative method of nanoparticle assembly which can be used to study these effects is the Langmuir−Blodgett (LB) technique.[34−37] The LB technique takes advantage of the ability to fully and evenly disperse the particles on a compatible surface to generate a monolayer. The interparticle distance in the monolayer can be changed (and thus modulate the near-field surface coupling) by changing the LB pressure prior to depositing the monolayer.

Conjugated polymers have been studied extensively for their use in electronic devices as well as sensory applications because of their strong absorption, emission, and conducting properties.[38−40] When in the condensed phase, there is an increased probability of interaction between chains at short distances, which results in an increased number of diffusion pathways of the exciton. Within the polymer matrix, the increased mobility of the excitons leads to a greater likelihood of exciton−exciton interaction. A possible result of this interaction is an annihilation process in which one exciton is excited to a higher excited state at the expense of the other, which is deactivated nonradiatively to the ground state. This annihilation process has been observed often with the high rates of excitation intensity of pulsed lasers.[41−44]

In the present work, we used a relatively weak continuous wave excitation source to excite the PPE fluorescent polymer that has been deposited by the LB technique over a monolayer of silver nanocubes (AgNCs) of different surface densities and thus have different surface plasmon field strengths. The LB technique was used to assemble the PPE fluorescent polymer into a monolayer on the top of AgNCs. This method of arrangement serves to limit the three-dimensional layer-to-layer interaction between the PPE fluorescent polymer matrix. This results in a less complicated architecture compared to casting methods.

It was observed that as the nanocube surface density increased, the fluorescence intensity of the polymer first increased. As the surface density of the nanoparticles is increased further, the fluorescence began to decrease rapidly. These results are discussed in terms of the changes in the surface plasmon field strength of the assembled AgNCs, which enhanced the polymers' rate of absorption. Initially, this enhancement leads to an increase in the fluorescence intensity. Then, as the field strength greatly increased, the exciton density increases to a level where its collision rate, and thus the biexciton nonradiative annihilation processes, exceeded the polymer fluorescence rate and the observed polymer fluorescence intensity decreased rapidly.

Experimental Section

The synthesis of the PPE fluorescent polymer is discussed in detail within the Supporting Information. Briefly, the PPE fluorescent polymer synthesis began with the preparation of the fundamental building blocks, as shown in Scheme 1 (Supporting Information). Palladium-catalyzed coupling of monomers **1** and **2**

(19) Kerker, M. *J. Colloid Interface Sci.* **1985**, *105*, 297.
(20) Creighton, J. A.; Eadon, D. G. *J. Chem. Soc.-Faraday Trans.* **1991**, *87*, 3881.
(21) Creighton, J. A.; Blatchford, C. G.; Albrecht, M. G. *J. Chem. Soc., Faraday Trans. 2* **1979**, *75*, 790.
(22) Moskovits, M. *Rev. Mod. Phys.* **1985**, *57*, 783.
(23) Camden, J. P.; Dieringer, J. A.; Wang, Y.; Masiello, D. J.; Marks, L. D.; Schatz, G. C.; Van Duyne, R. P. *J. Am. Chem. Soc.* **2008**, *130*, 12616.
(24) El-Sayed, I. H.; Huang, X.; El-Sayed, M. A. *Nano Lett.* **2005**, *5*, 829.
(25) Neretina, S.; Qian, W.; Dreaden, E. C.; El-Sayed, M. A.; Hughes, R. A.; Preston, J. S.; Mascher, P. *Nano Lett.* **2009**, *9*, 1242.
(26) Biesso, A.; Qian, W.; El-Sayed, M. A. *J. Am. Chem. Soc.* **2008**, *130*, 3258.
(27) Biesso, A.; Qian, W.; Huang, X. H.; El-Sayed, M. A. *J. Am. Chem. Soc.* **2009**, *131*, 2442.
(28) Jensen, T. R.; Duval, M. L.; Kelly, K. L.; Lazarides, A. A.; Schatz, G. C.; Van Duyne, R. P. *J. Phys. Chem. B* **1999**, *103*, 9846.
(29) Reinhard, B. M.; Siu, M.; Agarwal, H.; Alivisatos, A. P.; Liphardt, J. *Nano Lett.* **2005**, *5*, 2246.
(30) Fromm, D. P.; Sundaramurthy, A.; Schuck, P. J.; Kino, G.; Moerner, W. E. *Nano Lett.* **2004**, *4*, 957.
(31) Tabor, C.; Murali, R.; Mahmoud, M.; El-Sayed, M. A. *J. Phys. Chem. A* **2009**, *113*, 1946.
(32) Huang, W. Y.; Qian, W.; Jain, P. K.; El-Sayed, M. A. *Nano Lett.* **2007**, *7*, 3227.
(33) Fischer, U. C.; Zingsheim, H. P. *J. Vac. Sci. Technol.* **1981**, *19*, 881.
(34) Mahmoud, M. A.; El-Sayed, M. A. *Nano Lett.* **2009**, *9*, 3025.
(35) Tao, A.; Kim, F.; Hess, C.; Goldberger, J.; He, R. R.; Sun, Y. G.; Xia, Y. N.; Yang, P. D. *Nano Lett.* **2003**, *3*, 1229.
(36) Tao, A.; Sinsermsuksakul, P.; Yang, P. *Nat. Nanotechnol.* **2007**, *2*, 435.
(37) Huang, J. X.; Kim, F.; Tao, A. R.; Connor, S.; Yang, P. D. *Nat. Mater.* **2005**, *4*, 896.
(38) Bunz, U. H. F. *Acc. Chem. Res.* **2001**, *34*, 998.
(39) Feng, F. D.; He, F.; An, L. L.; Wang, S.; Li, Y. H.; Zhu, D. B. *Adv. Mater.* **2008**, *20*, 2959.
(40) McQuade, D. T.; Pullen, A. E.; Swager, T. M. *Chem. Rev.* **2000**, *100*, 2537.
(41) Holzer, W.; Penzkofer, A.; Stockmann, R.; Meysel, H.; Liebegott, H.; Horhold, H. H. *Synth. Met.* **2001**, *125*, 343.
(42) Cerullo, G.; Lanzani, G.; De Silvestri, S.; Egelhaaf, H. J.; Luer, L.; Oelkrug, D. *Phys. Rev. B: Condens. Matter Mater. Phys.* **2000**, *62*, 2429.
(43) Kepler, R. G.; Valencia, V. S.; Jacobs, S. J.; McNamara, J. J. *Synth. Met.* **1996**, *78*, 227.
(44) Yan, M.; Rothberg, L. J.; Papadimitrakopoulos, F.; Galvin, M. E.; Miller, T. M. *Phys. Rev. Lett.* **1994**, *73*, 744.

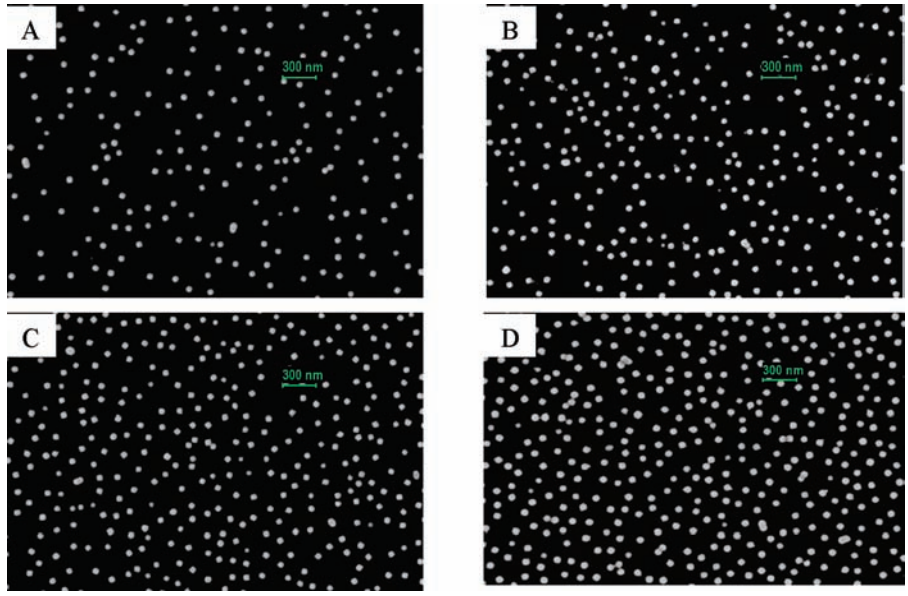

Figure 1. (A−D) SEM images of PVP-capped AgNC monolayers that have been assembled on silicon substrates at surface coverage of 5.7, 9.0, 10.7, and 13.8%, respectively. From these images, a monodisperse population of AgNCs was observed with an average particle diameter of 58 nm (SD = 6 nm).

furnished PPE **3**, which was reacted with *unsym*-dimethylethylenediamine to furnish PPE **4**. Upon reaction with iodomethane, PPE **5** resulted as an orange powder. According to gel permeation chromatography (GPC) vs polystyrene, the PPE has a molecular weight (M_n) and polydispersity index (PDI) of 1.1×10^4 and 1.95, respectively.

The silver nanocubes were prepared by heating 30 mL of ethylene glycol (EG) at 150 °C for 1 h.[17,45,46] EG was the solvent for all subsequent solutions in this synthesis. The heating of the EG was followed by the addition of a solution of polyvinylpyrolidone (0.28 g dissolved in 10 mL of EG) which had a molecular weight of ~55 000. The resulting solution temperature was adjusted back to 150 °C. Next, sodium sulfide (0.4 mL, 3 mM) was added and followed subsequently by the slow injection of silver nitrate (3.6 mL, 282 mM) into the reaction mixture. The silver ions were reduced completely after 15 min, producing AgNCs. For the purification of AgNCs, 5 mL of the AgNC solution was diluted with acetone, centrifuged, and then redispersed in water. Lastly, the particles were centrifuged again and dispersed in 10 mL of chloroform.

The AgNCs were assembled with the use of a Nima 611 D trough. First, 0.5 mL aliquots of AgNCs in chloroform were sprayed over the surface of the water-filled trough. Time was then allowed for the chloroform to fully evaporate, leaving the particles uniformly dispersed on the sublayer. The surface pressure was monitored with the use of a Wilhelmy plate, attached to a D1L-75 model pressure sensor. A mechanical barrier in contact with the surface was then closed to achieve increased surface pressures. These pressures were changed to attain variation in the percent of the surface coverage by the nanoparticles. A motorized dipper was used to deposit the AgNCs on a quartz or silicon substrate by drawing it through the floating monolayer. Using the same deposition procedure with a clean sublayer, a layer of the PPE fluorescent polymer derivative and PVP (360K or 10K), dissolved in chloroform, were then deposited onto the nanoparticle array at constant surface pressure. All polymer and AgNC deposits were taken from the same monolayer to ensure uniform assembly. The samples were characterized before and after deposition of the polymer.

Absorbance and steady-state fluorescence measurements were taken on an Ocean Optics HR4000Cg-UV-NIR absorption spectrometer and a Craic 100 microfluorescence spectrometer, respectively. The fluorescence was taken in reflectance mode through a 20× objective lens and excited with 400 nm light from a mercury-arc lamp. A power dependence study was conducted using neutral density filters to systematically reduce the intensity of the excitation source. For the lifetime measurements, frequency-doubled Ti:sapphire laser pulses at 400 nm were used to excite the sample on an inverted microscope, through a 60× water immersion objective. After passing through a monochromator, the emitted photons were detected with an MCP-PMT and recorded using a single photon counting board. Images were taken on a Zeiss Ultra60 SEM to determine the size, monodispersity, and percent surface-coverage of the particles. Lastly, a Picoscan 5 molecular imaging AFM was used for surface profiling.

Results and Discussion

Imaging of the AgNC Monolayer before and after Deposition of the PPE Polymer. Scanning electron microscopy (SEM) was used to characterize the morphology of the silver nanoparticle samples that were assembled on the surface of silicon substrates. The surface coverage (which determines the monolayer surface density and thus interparticle distance) changed as a function of the surface pressure at which the particles were deposited onto the substrate. AgNCs were assembled on both quartz and silicon substrates at surface pressures of 6, 5, 4, 3, 1, 0.5, and 0 mN/m. Figure 1 shows the SEM images of four of these samples, which were assembled at surface pressures of 6, 4, 1, and 0 mN/m. SEM imaging, which produced good images of the size and morphology of the monolayer, also allowed for the calculation of the percent of surface coverage and the average interparticle distance. From the SEM images, the distribution in size was determined to be monodisperse with an average edge length of 58 nm (SD = 6 nm). The surface coverage was found to be 5.7, 6.5, 9.0, 10.1, 10.7, 11.2, and 13.8% for the samples assembled at pressures of 0, 0.5, 1, 3, 4, 5, and 6 mN/m, respectively.

Although SEM produced a good description of the morphology of the monolayer in two-dimensions, atomic force micros-

(45) Mahmoud, M. A.; Tabor, C. E.; El-Sayed, M. A. *J. Phys. Chem. C* **2009**, *113*, 5493.
(46) Siekkinen, A. R.; McLellan, J. M.; Chen, J. Y.; Xia, Y. N. *Chem. Phys. Lett.* **2006**, *432*, 491.

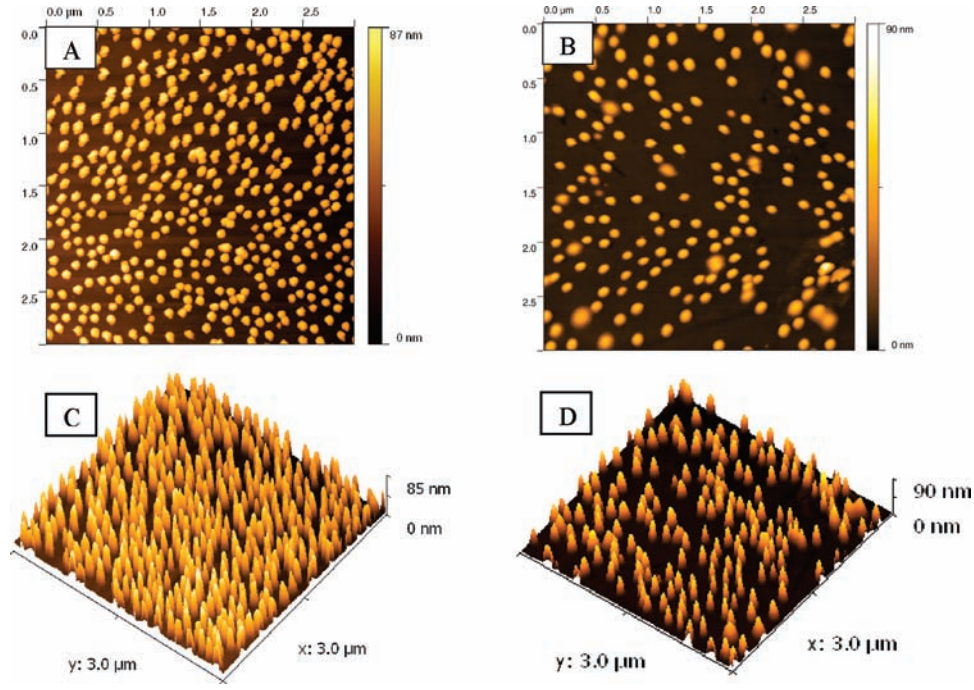

Figure 2. AFM 2D and 3D representations of monolayers of PVP-capped AgNCs that have been deposited on quartz substrates and covered with a thin layer of PPE polymer. AgNCs were assembled to surface coverage of 13.8% (A and C) and 5.7% (B and D). AFM measurements give a particle-plus-polymer diameter of 65 nm. Combining AFM and SEM measurements, the thickness of the PPE polymer that was deposited onto the nanoparticle monolayer was determined to be ~7 nm.

copy (AFM) was used to gain insight into the monolayer topography. Contrary to the SEM, the AFM images contain details relating to both the polymer and the AgNCs. Figure 2 shows the AFM images of AgNC monolayers that were coated with PPE polymer after being assembled to surface coverages of 13.8% (Figure 2A,C) and 5.7% (Figure 2B,D). The 2D image view of AgNC monolayers corresponds well with the SEM images in terms of particle arrangement. This means that the monolayer did not change during the deposition of the PPE polymer layer. The thickness of the polymer layer was calculated from the *z*-component of the AFM topographic images shown in Figure 2B,C. According to the SEM images, the edge length of the AgNC is 58 nm. The height of the AgNC−polymer structures, in Figure 2C,D, is determined to be 65 nm, yielding a polymer thickness of ~7 nm.

Statistical Analysis of the Average Interparticle Distance as a Function of Surface Pressure. The average center-to-center interparticle distance was determined, from nearest neighbor particle measurements within the SPIP image analysis software, and found to range from 157 to 130 nm (from 5.7% to 13.8% coverage). The center-to-center interparticle distance was the mean value taken from the distribution of particle pairs. These distributions are displayed in Figure 3 as a series of histograms that show a shifting of the particle pair population to smaller interparticle separations. More significant than the separation, the distributions show a narrowing of the population (described by the values of the standard deviation) and a continued increase in the number of particle pairs from low surface coverage to higher coverage.

An interesting progression of the particle distributions, which is characteristic of LB monolayers, can be seen in Figure 3A−D. The low surface coverage sample (A) shows a broad distribution of randomly oriented particles, which is referred to as the "gas phase" when assembling monolayers on the LB trough.[18] The samples ranging from 9.0% to 10.7% coverage (B−D) show a narrowed population, and the distribution is tending toward a lower interparticle separation. This increased region of compression is the "liquid phase", since the particles are adopting a condensed arrangement with greater order. Lastly, the highest surface coverage samples (E and F) can be related to the "solid phase", because of the noticeably more narrow distribution and increased concentration of particles. It is the combined effect of the proximity and the density of particles at such close distances and the extent of multiparticle coupling that is responsible for the large enhancements of particle near-fields. The decrease of the interparticle separation occurs as the particles are spatially influenced by an increasing number of neighbors that are forced into the same area (at higher surface pressures) during the assembly by the LB trough. This also leads to a narrowing of the distribution due to the restricted movement of the particles. Overall there are many more particles interacting at close and similarly spaced proximities when the surface pressure is continually increased.

Plasmon Spectra of AgNCs and AgNCs Coated with PPE Polymer. Silver nanocubes have three surface plasmon spectral peaks.[45] Figure 3A shows the surface plasmon resonances of 58 nm AgNCs that were capped with PVP and deposited into monolayers that have been assembled to surface coverages of 5.7, 6.5, 9.0, 10.1, 10.7, 11.2, and 13.8%. The dipolar coupling of neighboring AgNC particles led to a decrease in the plasmon oscillation frequency and thus gave the observed red-shift as the surface coverage increased (Figure 4A).[18] Although the SPR spectral position of AgNCs are red-shifted as the interparticle separation distance decreases (increasing the percent of coverage area), the absorption spectrum of the PPE polymer strongly interacts with the primary plasmon peak of each AgNC sample, which exhibits a maximum shift of ~18 nm (see Figure 4B). Additionally, a uniform red-shift of 5−7 nm was observed for the lowest energy peak upon deposition of the PPE polymer onto the AgNC arrays. This shift was due to the change in the

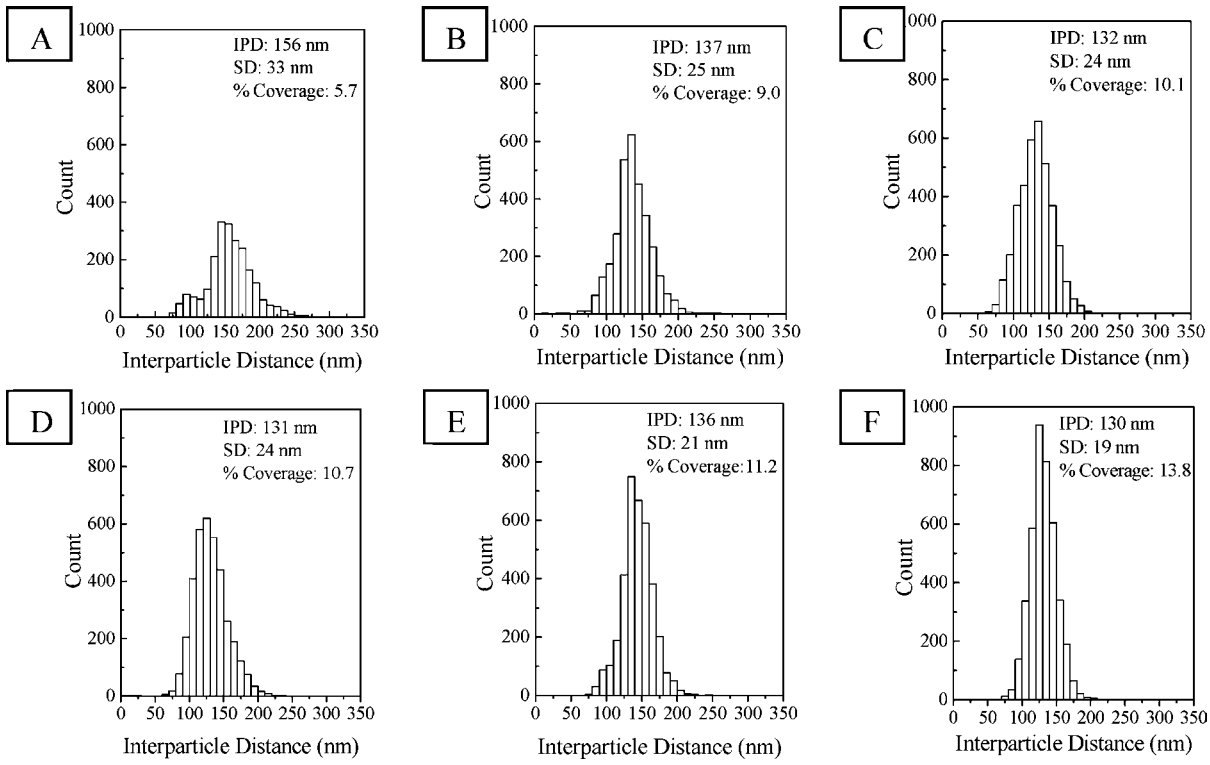

Figure 3. Distribution of nearest neighbor AgNC interparticle distances within each sample assembled on the LB trough at different surface pressures: (A) 5.7%, (B) 9.0%, (C) 10.1%, (D) 10.7%, (E) 11.2%, and 13.8%. The distribution of particles narrows and shifts to lower interparticle distance, and the number of particle pairs increases as the percent coverage is increased. The 6.5% coverage is not shown due to its similarity to the 5.7% coverage sample, with the exception of yielding a higher number of particles pairs.

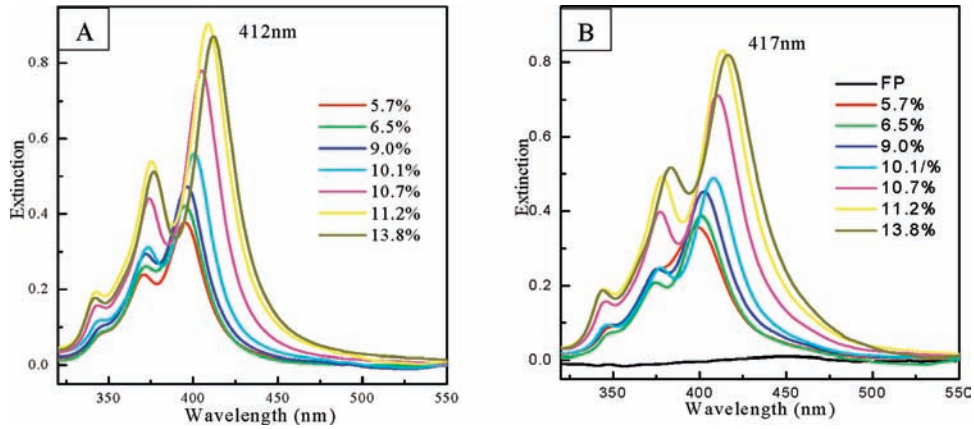

Figure 4. UV−visible plasmonic extinction spectra of PVP -capped AgNC monolayers that have been deposited on quartz substrates, at varied surface coverage, before (A) and after (B) coating with a ∼7 nm layer of PPE polymer. Before polymer coating, a progressive red-shift was observed as the interparticle coupling increased. After deposition of the polymer, a uniform 5−7 nm red-shift is observed in each spectrum due to the change in the local dielectric environment of the particle.

local dielectric environment of the particles as the polymer was deposited onto its surface.

To confirm that a uniformly random distribution of the PPE polymer is present around the AgNC monolayers, polarized florescence measurements were conducted. This experiment showed no change in the fluorescence peak intensity or shape with monitoring of polarized emission. Additionally, SERS measurements showed no observable deviation in the Raman peaks position or intensity as a function of changing polarization of the exciting light. The results of the polarized fluorescence and SERS experiments suggest that there is no indication that the film has a preferred molecular orientation or arrangement that could affect our results, and therefore, the PPE film is assumed to be uniformly randomly oriented.

Steady-State Fluorescence of Pure PPE Polymer Deposited on AgNC Monolayers as a Function of Langmuir−Blodgett Surface Pressure. Figure 5A shows the absorption spectra of the PPE films deposited onto quartz substrates at different surface pressures. As the surface pressure increased, the degree of compression and, as a result, the amount of polymer in the spectrometer monitoring beam cross-section increased as is indicated by the absorbance at 436 nm (Figure 5A). Figure 5B shows the steady-state fluorescence of the PPE polymer films excited at 400 nm. The fluorescence intensity also increased as

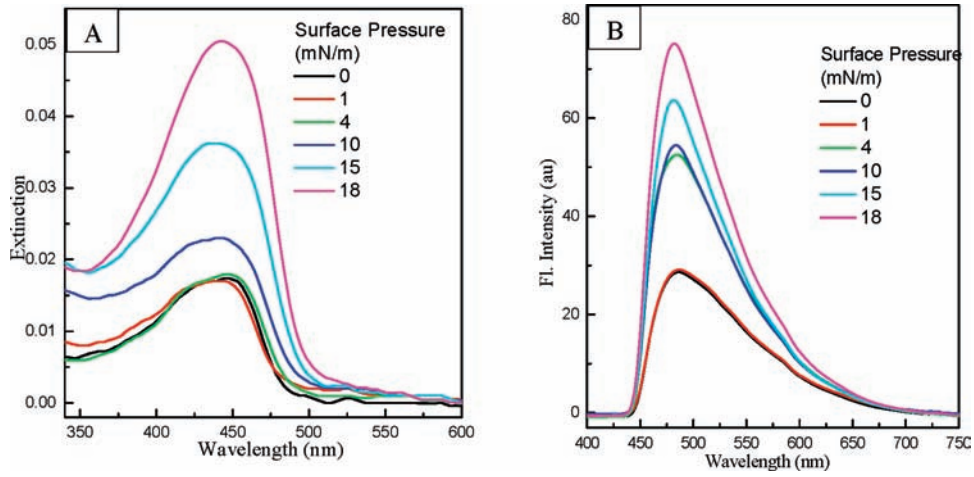

Figure 5. (A) The UV−visible extinction spectra of PPE polymer films deposited by the LB trough onto quartz substrates at surface pressures of 0, 1, 4, 10, 15, and 18 mN/m. (B) The corresponding steady-state fluorescence; $\lambda_{ex} = 400$ nm. In the case of the pure polymer, the extinction and fluorescence intensities both increased by increasing the surface pressure.

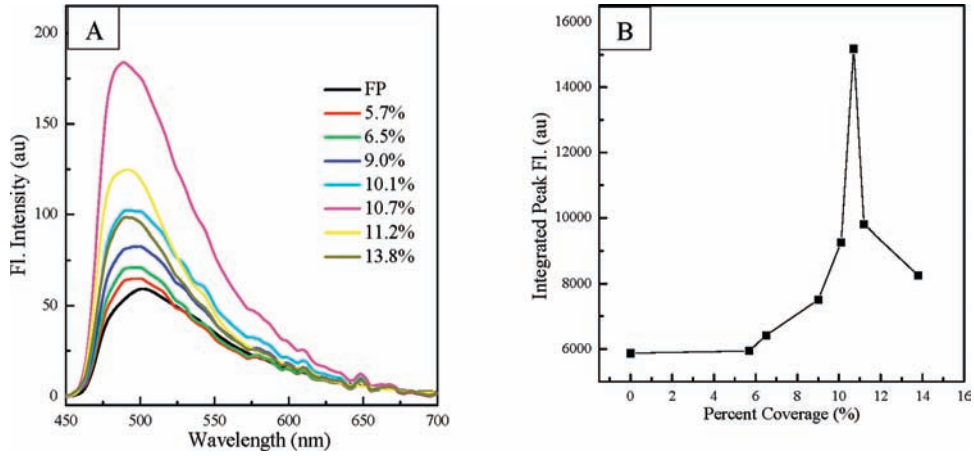

Figure 6. (A) Steady-state fluorescence spectra of PPE fluorescent polymer covering PVP-capped AgNC monolayers that have been deposited onto quartz substrates to different surface coverage. (B) The relationship between the integrated peak intensity and the surface coverage by AgNCs illustrates the dramatic decrease in the fluorescence intensity that is observed at a surface coverage of 11.2% and beyond.

the absorption peak intensity increased. The increased number density of the molecules compressed into the beam is expected to increase the absorption and the fluorescence intensity

The steady-state fluorescence of the AgNC−PPE samples that were assembled at different surface coverage is shown in Figure 6A. The trend is shown graphically in Figure 6B, in which the integrated fluorescence band intensity increases, with increasing coverage, to a maximum value at a surface coverage of 10.7% and then decreases sharply. The fluorescence intensity prior to the rapid decrease shows a fluorescence enhancement of 260% over that of the pure polymer. Both the intensity increase prior to the 10.7% coverage and the quenching phenomenon observed thereafter are proposed to result from the increase in the surface plasmon fields of the AgNC monolayer associated with increasing the nanoparticle density. In these experiments, the plasmonic particles have inhomogeneous separation distribution. Once the interparticle distance reaches a range that enhances the electromagnetic field of the exciting light, surface plasmon enhanced polymer excitation occurs and the fluorescence is enhanced. Additional increase in the field enhancement results in an increase in the exciton densities that initiate exciton annihilation. When this occurs, the fluorescence intensity decreases as the rate of annihilation exceeds the rate of the enhanced fluorescence. The rapid decrease due to annihilation is proportional to $I^2C^2\sigma$, where I is the lamp intensity, C is the plasmonic enhancement factor, which is very sensitive to the interparticle separation, and σ is the fraction area of the excited spot that contains nanoparticles of equal or smaller separation than the critical distance. At or below this critical distance surface fields are large enough to allow the rate of annihilation to compete with the fluorescence rate. Because the distribution of the nanoparticles separation in the monolayer is inhomogeneous (see statistical analysis of interparticle distances shown in Figure 3), there are particles separated by distances that induces such large fields (smaller distance) and those that are not (larger distance). As the surface pressure is increased, the value of σ increases due to the increasing number of particles that have the critical distance where the surface fields are strong enough to increase the rate of their absorption. This increases exciton densities, resulting in a rate of annihilation that is larger than that of the fluorescence. This results in an increase of the percentage of the surface being involved in the effective rate of annihilation that decreases the fluorescence intensity. At high enough pressures, at which all the neighboring particles have distances equal or shorter than the critical distance, saturation could be observed.

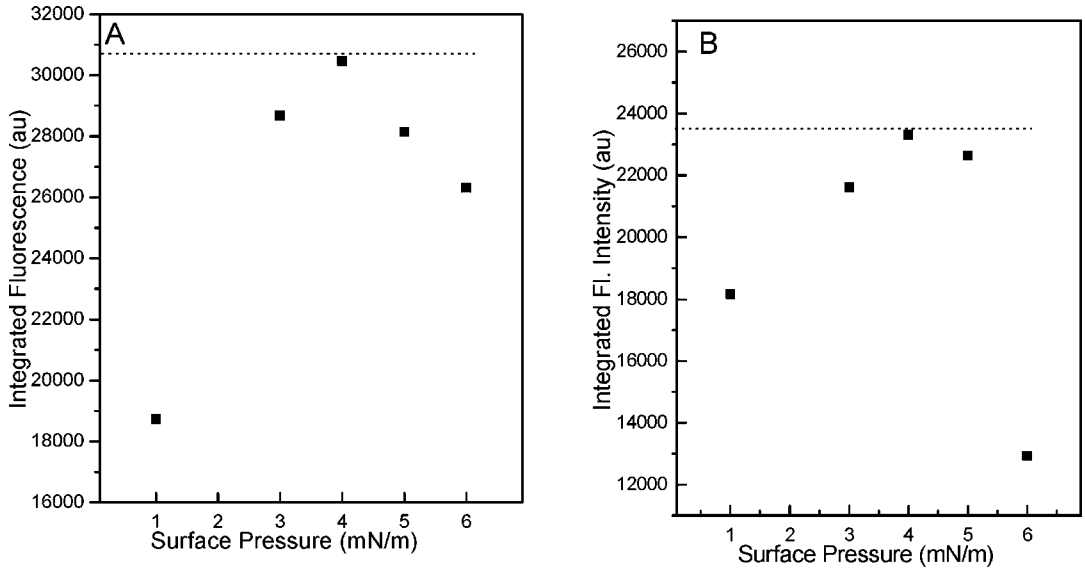

Figure 7. Integrated band intensities taken from the fluorescence spectra of PPE polymer monolayer separated from the AgNC monolayer with spacer layers of PVP with molecular weights of (A) 360 000 and (B) 10 000. In both cases, the fluorescence intensity first increases at low surface pressure, where a turning point occurs, and the fluorescence intensity begins to drop at the higher surface pressures. However, the annihilation sets in earlier at the closer distances (B) from the plasmonic field, limiting the maximum of the fluorescence intensity to a lower value (23 000 au) instead of the 30 000 au value observed at larger separation. This is consistent with plasmonic field effects on the polymer absorption rate.

Steady-State Fluorescence Enhancement of PPE Polymer Monolayers at Different Separations from the AgNC Monolayer. In order to further support that our observations result from changing the plasmon field effect and eliminate a possible mechanism involving either the effect of the metallic nanoparticles in the polymer configuration or charge transfer processes from the polymer to silver nanoparticles, we carried out an experiment in which the silver monolayers are separated from the fluorescent polymer by different distances. This was accomplished by depositing monolayers of PVP with different molecular weights. Molecular weights of 360K and 10K were used to obtain different spacer thickness. The integrated fluorescence band intensities of PPE polymer are shown in Figure 7 for (A) 360K and (B) 10K PVP spacer layers as the surface pressure of the AgNC monolayer is varied. In both cases the fluorescence increased significantly and then decreased at higher surface pressure. This, along with the other fluorescence data presented in this paper, seems to suggest that the observed fluorescence intensity increase and subsequent decrease occur regardless of modifications made herein to the separation between AgNC and PPE polymer layers. From our experience that plasmonic fields increase the radiative properties of nearby electronic systems,[47] one concludes that the rate of the polymer absorption increases, leading to increased fluorescence. Further increase leads to enhanced rates of exciton collision and increased annihilation rates, which decrease the fluorescence intensity. In both cases of Figure 7, the fluorescence intensity first increases then decreases. At the larger separation distance from the AgNC plasmonic layer, provided by the 360K PVP, the fluorescence intensity decrease sets in after a maximum fluorescence of ~30 000 au was reached. When the smaller molecular weight PVP (10K) is used to separate the AgNC monolayer from the PPE polymer layer by a smaller distance, a maximum fluorescence intensity of only ~23 000 au is reached. Thus, at smaller distance from the plasmonic field, the annihilation sets in earlier and does not allow the enhanced fluorescence to continue to increase to the same extent that was observed with the 360K spacer. This also supports the proposal that the plasmonic field led to enhancing the absorption and subsequently the annihilation.

Fluorescence Lifetime of Pure PPE Polymer and PPE Polymer Deposited on AgNC Monolayers. The changes in plasmon field effects of the AgNC particles altered the steady-state fluorescence emission intensity, as discussed in the previous section. Figure 6A shows the fluorescence decays of the PPE polymer films that were assembled at different surface coverage. The decays were all biexponential, which is typical of concentrated samples of PPE derivatives.[48] Figure 8B summarizes the deconvoluted fluorescence decays, the long (top) and the short (bottom) components, as the surface coverage increased. The fluorescence lifetimes of the pure polymer sample (1.19/0.39 ns) were longer than that of any of the AgNC−PPE samples, while the shortest lifetime was observed from the 10.7% surface coverage sample (0.89/0.28 ns).

The small changes in the observed lifetimes do not correspond to the large observed decrease in the steady-state fluorescence intensity. The observed drop in intensity that was observed at 11.2% coverage was not accompanied by any change in the corresponding lifetimes. This can be explained by considering how the lifetime experiment is conducted and how steady-state measurements are carried out. When the fluorescent polymer is excited by a pulsed laser in the lifetime experiment, the plasmonic field is only present during the initial excitation pulse width as it decays very rapidly. Thus, the observed decay takes place in the absence of any plasmonic excitation of the nanoparticle. Thus, it is not surprising that the lifetimes are not greatly affected.

Excitation Power Dependence of the Fluorescence Intensity. In standard experiments involving exciton−exciton annihilation, an intense pulsed laser is usually used and the pulse intensity

(47) Neretina, S.; Qian, W.; Dreaden, E.; Ei-Sayed, M. A.; Hughes, R. A.; Preston, J. S.; Mascher, P. *Nano Lett.* **2008**, *8*, 2410.

(48) Bunz, U. H. F.; Imhof, J. M.; Bly, R. K.; Bangcuyo, C. G.; Rozanski, L.; Bout, D. A. V. *Macromolecules* **2005**, *38*, 5892.

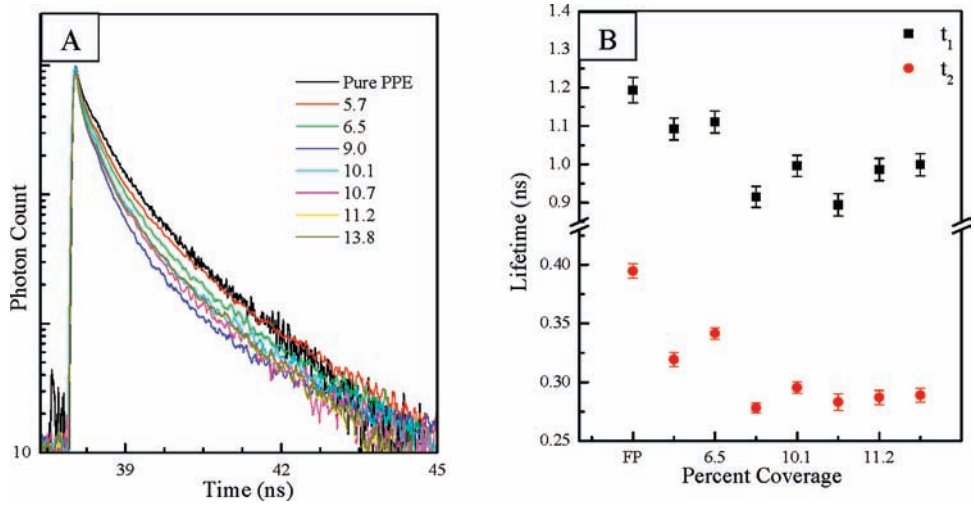

Figure 8. (A) Fluorescence intensity decay measurements of pure PPE polymer (black) and PPE polymer on the surface of PVP-capped AgNC monolayers that have been deposited onto quartz substrates at different surface coverage. (B) The dependence of the long (top) and the short (bottom) decay components of the deconvoluted fluorescence decay of the polymer as a function of surface coverage of the AgNCs on which the polymer was deposited.

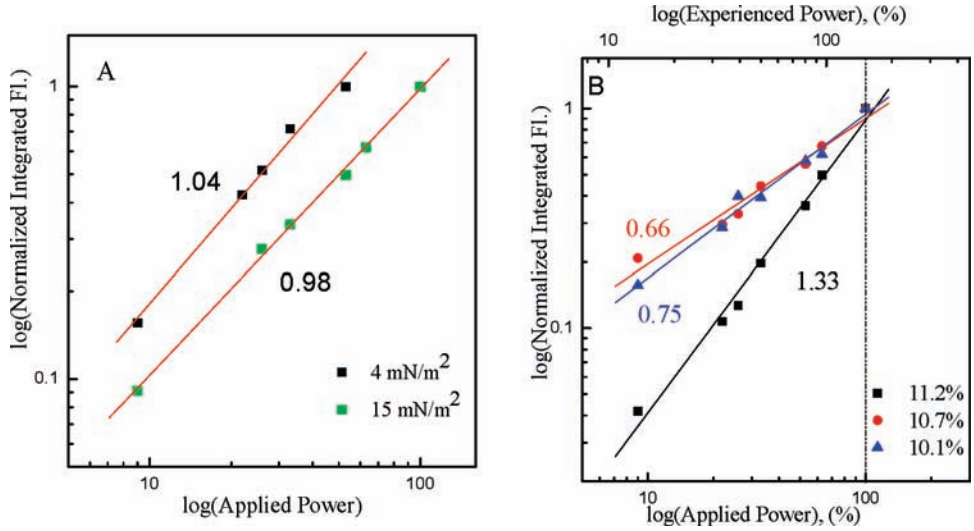

Figure 9. Logarithmic plots of the excitation power plotted against the integrated fluorescence intensity of (A) pure polymer samples that were deposited onto quartz substrates at surface pressures of 4 mN/m (black) and 15 mN/m (green), as well as (B) PPE fluorescent polymer deposited on the surface of PVP-capped AgNC monolayers on quartz substrates at different surface coverage. Samples with 11.2% (black), 10.7% (red), and 10.5% (blue) coverage show altered slopes that indicate that the polymer is experiencing fluorescence enhancement in each sample but is undergoing the two-photon process of exciton annihilation in the 11.2% surface coverage sample.

is varied over a large range of energy densities. At higher light densities the fluorophore is generating large numbers of excitons, which can ultimately come into close contact to annihilate each other and reduce the amount of the observed fluorescence per unit energy of the pulse.[41] Exciton−exciton annihilation has been observed previously in thin films of fluorophores.[41,49−51] Keplar observed this annihilation process in PPV thin films excited with high-fluence pulsed lasers and decreases of up to 70% of the original fluorescence yield.

Figure 9A shows how the intensity of the PPE polymer fluorescence, in the absence of AgNCs, changed with the exciting light intensity for surface pressures of 4 and 15 mN/m. The linear dependence was expected for both samples as singlet−singlet annihilation does not typically take place in the pure polymer sample at the continuous wave lamp intensities used. When the PPE polymer was excited after it had been deposited on the nanocubes, the situation was again different. At low surface coverage of nanocubes, the excitation dependence was linear with a slope of 0.66. At high silver nanocube surface coverage, the fluorescence was again linear, but with a slope of 1.33. The roughly doubled slope, from the sample at 10.7% coverage to that at 11.2% (figure 9B), suggests that a multiphoton process was occurring on the surface of the excited nanocubes. The reason that the slopes of the 10.7 and 10.1% AgNC−polymer samples were smaller than that the polymer alone (Figure 9A) could be a result of the surface plasmon field-enhancement of the rate of polymer absorption. The AgNCs increased the rate of the absorption of the polymer due to the field enhancement of the intensity of Hg light used, which leads

(49) Cerullo, G.; Lanzani, G.; De Silvestri, S.; Egelhaaf, H. J.; Luer, L.; Oelkrug, D. *Phys. Rev. B* **2000**, *62*, 2429.
(50) Kepler, R. G.; Valencia, V. S.; Jacobs, S. J.; McNamara, J. J. *Synth. Met.* **1996**, *78*, 227.
(51) Yan, M.; Rothberg, L. J.; Papadimitrakopoulos, F.; Galvin, M. E.; Miller, T. M. *Phys. Rev. Lett.* **1994**, *73*, 744.

to an apparent excitation intensity that is lower than the actual excitation experienced by the polymer.

In order to demonstrate this enhancement of the absorption efficiency of the polymer, the scale on the *x*-axis (Figure 9A, top) was multiplied by a scalar value of 1.51 to reflect the amount of light necessary to elicit the same amount of fluorescence without the presence of AgNCs (i.e., the excitation dependence of the low coverage sample should have a slope of 1). The value of 1.51 is the square of the surface field enhancement factor of Hg light intensity. Thus, by correcting the intensity axis, the slope of the low coverage changes from 0.66 to 1 (a one-photon process). On the same corrected axis, the slope of the high particle coverage changes from 1.33 to 2 (a two-photon process). In effect, the polymer is "experiencing" a much higher intensity of light than what we are exposing it to due to the plasmon field enhancement. After this was carried out, it was obvious that the dependence of the fluorescence intensity on the exciting light was linear at low surface coverage (a one-photon process) and quadratic at high surface coverage (a two-photon process).

The next question is: how can we observe a continued increase in the fluorescence intensity with increasing exciting light intensity from a system that is undergoing two-photon annihilation processes? In the power dependence studies, the interparticle distance is held constant, which means that the percentage of the sample that has interparticle distances at or below the critical annihilation distance is held constant. Therefore, the rate at which annihilation occurs compared to the fluorescence enhancement rate remains relatively the same. Increasing the power of the lamp serves to inject additional excitons, which undergo the same ratio of fluorescence or annihilation to yield a linear increase in fluorescence intensity with power. In the annihilation process, one of the excited polymers gives fluorescence. Thus, increasing the rate of annihilation increases the fluorescence intensity.

Acknowledgment. The authors would like to thank Dr. Lawrence Bottomley for helpful discussion. The authors would also like to thank the Airforce AFOSR—Center of Excellence on BIONIC * under grant No FA9550-09-1-0162.

Supporting Information Available: The synthesis of PPE polymer. This material is available free of charge via the Internet at http://pubs.acs.org.

JA907657J